Journal of Achievements in Materials and Manufacturing Engineering
VOLUME 55
ISSUE 2
December
2012

# Study of electroless nickel plating on PerFactory™ rapid prototype model

**J.C. Rajaguru, C. Au, M. Duke***
Faculty of Science and Engineering, University of Waikato, Hamilton, New Zealand
* Corresponding e-mail address: dukemd@waikato.ac.nz

Received 20.10.2012; published in revised form 01.12.2012

**Manufacturing and processing**

## ABSTRACT

This paper presents an investigation of electroless nickel plating on PerFactory™ rapid prototype model built on PerFactoryTM R05 material. PerFactory™ R05 is acrylic based photo sensitive resin. It is a popular material in rapid prototyping using PerFactory™ method which employs addictive manufacturing technique to build prototypes for visual inspection, assembly etc. Metallization of such a prototype can extend the application envelop of the rapid prototyping technique as they can be used in many functional applications. Unlike the electroless nickel plating on metal substrate, the process on acrylic resin substrate is not auto-catalytic. Hence, etching and activation are necessary for initiating the process. The final coating is then investigated using scanning electron microscope (SEM) together with energy dispersive spectroscopy (EDS) and x-ray diffraction (XRD) analysis to identify the morphology and structure of the coating. The SEM & EDS analysis on surface and chemical composition of model surface after each preliminary surface treatment are also presented. Finally the layer is tested on Vickers micro hardness tester.

**Keywords:** Rapid prototyping; Electroless nickel plating; Plastic coating

**Reference to this paper should be given in the following way:**
J.C. Rajaguru, C. Au, M. Duke, Study of electroless nickel plating on PerFactory™ rapid prototype model, Journal of Achievements in Materials and Manufacturing Engineering 55/2 (2012) 782-789.

## 1. Introduction

Rapid prototyping is a major addictive manufacturing technique and it has been used all over the world in manufacturing industries. Most of the rapid prototyping processes are based on polymerisation of a photo sensitive polymer in the presence of ultra violet or laser radiation. In contrast with the conventional subtractive manufacturing technologies, the prototypes are built directly from CAD file without any tooling or machining [1].

A CAD model is fed into the rapid prototyping machine controller and is layered to yield the two dimensional profiles to drive the UV or laser beam. The photo sensitive polymer in the rapid prototyping machine is in liquid form. The polymer solidifies under the exposures of UV laser to generate a prototype. The prototype is produced layer by layer [2] and is then post-cured under the intensive UV radiation or in a thermal chamber so that the uncured portions between the layers are completely polymerized [3]. This, in fact, significantly improves the engineering properties such as elongation to fracture, ultimate tensile strength, modulus of elasticity, etc [4] of the prototype.

The material properties of a rapid prototype are poor compared to other materials such as steel and aluminium. These weak mechanical and thermal properties hinder its further applications as a function prototype under loading and thermal conditions [5]. In order to widen the application envelop, metallization is applied to the prototype.

PerFactory™ rapid prototyping uses Digital Light Processing Technology to solidify acrylic base photo polymer using UV light in contrast to laser curing process of Stereolithography process. So energy consumption of the curing process in PerFactory™ rapid prototyping method is less compare to laser curing method.

Electroless nickel plating is widely used in industry to improve the mechanical properties such as wear resistance,

hardness, corrosion resistance of a metal. It is an auto catalytic chemical reaction under the influence of a reducing agent. Unlike the electroplating, electroless nickel plating produces a uniform layer of coating regardless of the geometry complexity [6-10]. Therefore, in order to widen the feasibility of a PerFactory™ rapid prototype for functional applications, electroless nickel plating is a possible candidate which coats a layer of nickel phosphorous alloy on the prototype sample which improves the mechanical and thermal properties.

The electroless nickel plating on metal substrate is an auto-catalytic process. The metal substrate acts as a cathode to initiate the potential between the solution interface and substrate. However, the process is no longer auto-catalytic for non-metal. As a result, the plating process has to be activated chemically by the noble metal such as palladium.

The electroless nickel plating process has been successfully applied on many metallic substrates and some non-metallic substrates such as thermoplastic acrylonitrile butadience styrene [11,12], glass microsphere [13], silicon [14] etc. The major challenge for plating the non-metallic substrate is to attract the nickel ions. The deposition will continue once started because the deposited nickel acts as the catalyst. In order to attract the nickel ion, the non-metal substrate needs to have good hydrophilicity for seeding the noble metal to activate the process.

This paper investigates electroless nickel coating on the R05 rapid prototype model. According to the authors' knowledge, there is no literature pertaining to perform electroless nickel plating on PerFactory™ rapid prototype model built on R05 acrylic base photopolymer, which is a major material for PerFactory™ rapid prototyping. Coating a layer of nickel on the prototype can greatly improve its mechanical and thermal properties and expands its engineering applications.

## 2. Experiment

Substrates for electroless nickel plating are models built by a PerFactory SXGA Standard UV machine from Envision Tech GmbH [16]. The samples are built at Z vowel thickness of 45µm. The material used to build the sample is R05 liquid photo reactive acrylic resin. Some of the thermal and mechanical properties of PerFactory™ R05 material are tabulated in Table 1.

The steps involved in the plating process can be divided in to five sub-processes as given in Fig. 1. Electroless process conditions and concentrations for each preliminary pre-treatment are listed in Table 2.

First, PerFactory™ model surface is degreased by sodium hydroxide (NaOH) for 5 minutes at room temperature and is dried after rinsing with water. Then surface of the sample are etched with chromic acid solution ($H_2SO_4$ and $CrO_3$) for 5 minutes at room and it is dried after rinsing with plenty of water. Under sensitization, the surface is wetted by immersing in stannous chloride ($SnCl_2$) solution for 1 minute. Then the surface is activated by dipping the sample into palladium chloride ($PdCl_2$) solution for 5 minutes. Both stannous chloride and palladium chloride solution are prepared dissolving in hydrochloric acid (HCl). Finally, the electroless solution is prepared using nickel sulphate hexahydrate ($NiSO_46H_2O$) and sodium hypophosphite ($NaH_2PO_2$). The surface is immersed into the electroless solution at temperature of 80°C. The pH value of the solution is maintained at 7. The experimental setup is placed inside a fume hoop and is set to run mixing sodium hypophosphite.

Table 1.
R05 PerFactory™ resin property [15]

| Property | Measure |
|---|---|
| Tensile strength | 49.9 MPa |
| Glass transient temperature | 120-150ºC |
| Hardness (Shore D) | 86 |
| Density | 1.215 g/cm$^3$ |
| Flexural Strength | 79.7 MPa |
| Flexural Modulus | 1.96 GPa |

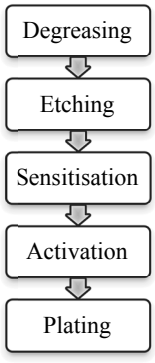


Fig. 1. Main steps in the electroless nickel plating

## 3. Result and discussion

The surface morphologies of the surface during pretreatment are investigated using Hitachi S4700 scanning electronic microscopic (SEM) and are shown in Fig. 2. During degreasing process, there is no significant different in the model surface morphology compare to original surface. However, after etching, the surface exhibits pit and oxidized rough morphology. That is similar to the increment of surface area with hole as reported by Alexandre et. al [16]. Those holes are generated due to the selective corrosion by sulfuric acid which enhance the seeding area for stannous and palladium ions. Further, those holes act as anchor points to adhere final nickel phosphorous layer to the substrate which is crucial achieving high degree adhesion layer to the PerFactory™ model.

Depth of those new opening are not visible. However, the presence of aluminum (Al) and silicon (Si) in the acrylic resin according to Fig. 2 shows the creation of new surface due to the new openings. After sensitizing and activation, there is no significant morphology change. But the EDS analysis using Noran System Six attached to SEM detect the chromium, stannous and palladium as extra possible element on the surface. The EDS spectra for pretreatment processes are presented in Fig. 3. This is a good indication of the presence of noble metal ions in a very low quantity to initiate the electroless process on surface of the model.

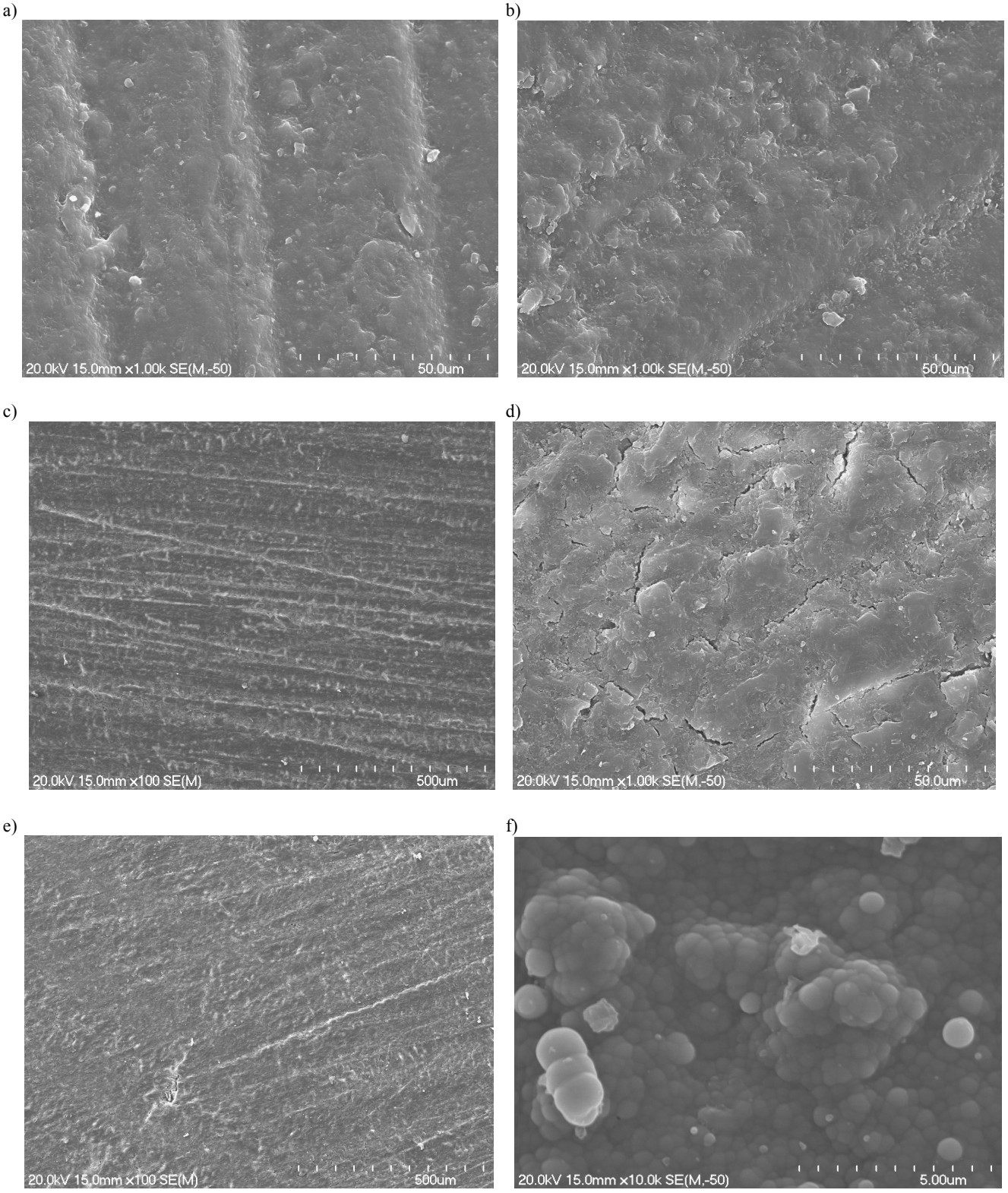


Fig. 2. The surface morphologies: a) original PerFactory$^{TM}$ model surface, b) surface after degreasing, c) surface after etching at 100 magnifications, d) surface after etching at 1000 magnification, e) surface after sensitising, f) surface after electroless nickel plating

Table 2.
Composition and conditions of the electroless nickel plating for acrylic resin

| Chemicals | Concentration | Condition |
|---|---|---|
| $NiSO_4.6H_2O$ | 40g/l | 80°C, pH 7, deionised water |
| $NaH_2PO_2$ | 20g/l | 80°C, pH 7, deionised water |
| $CrO_3$ | 1 g/l | Room temperature, Sigma Aldrich |
| $H_2SO_4$ | 98% | Sigma Aldrich, used as received |
| $SnCl_2$ | 1g | Room temperature |
| $PdCl_2$ | 0.1g | Room temperature, dissolved in HCl ,Sigma Aldrich |
| HCl | 36% | Room temperature |
| $H_2O$ | | Room temperature, deionised water |

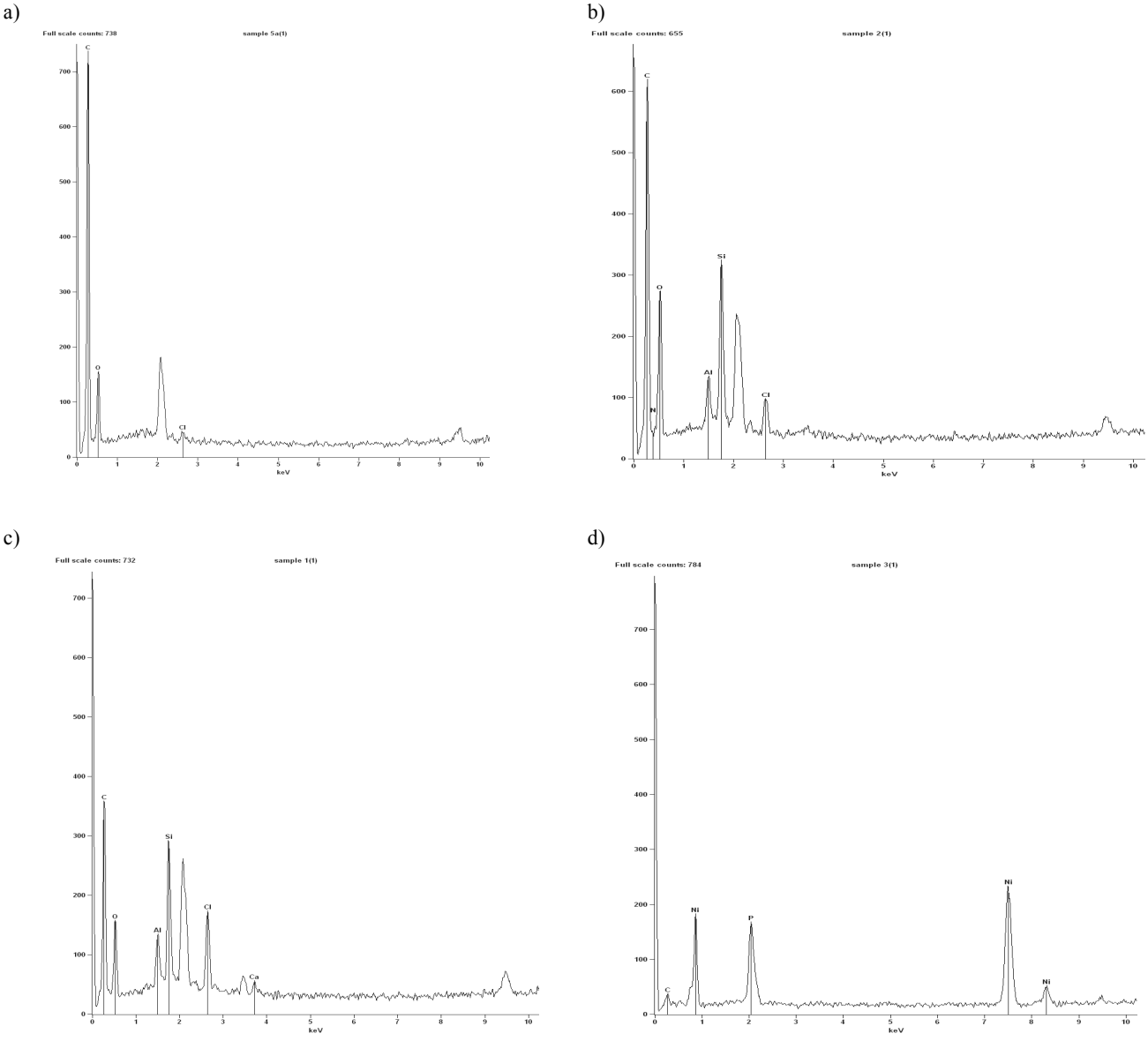


Fig. 3. The EDS spectra: a) original surface, b) after etching, c) after activation, d) after plating

The material is a non-metal and it does not attract the nickel ions during the electroless nickel plating process. As a result, the process is not auto-catalytic. In order to restore the nickel ion attraction on the acrylic resin substrate, preliminary treatments are necessary. The treatments include sensitization and subsequent activation of the acrylic resin by using the following solutions: sodium hydroxide, chromic acid, stannous chloride and palladium chloride. The etching by chromic acid makes the substrate hydrophilic so that it can be wetted by the stannous chloride. The substrate is sensitized by absorbing the tin ($Sn^{2+}$) ions from stannous chloride solution which reacts with the palladium ($Pd^{2+}$) ions during the activation process.

$$Sn^{2+} + Pd^{2+} \rightarrow Sn^{4+} + Pd \quad (1)$$

The electroless nickel plating cannot be activated without seeding of the palladium ions on the substrate surface. Fig. 2 f) shows the morphology of the final phase after electroless plating. It is resemble to a typical nickel phosphorous morphology and the corresponding EDS spectrum (Fig. 3 d) clearly indicates that the main components are nickel and phosphorous.

The EDS analysis shows that aluminium, silicon and chlorine are at low percentage of 1.9%, 6.0% and 3.7% respectively. Main components of acrylic resin are carbon, hydrogen and oxygen. But, hydrogen is undetectable because of the EDS machine limitation. Unmark peeks in EDS spectra correspond to platinum which is required to be sputtered on to the model surface to make it conductive. Nickel and phosphorous content of electroless layer are is 78% and 10.6% respectively. The layer thickness is calculated using gravity metric method. The mass of layer is calculated using digital weighing machine with five digit accuracy and area plated. The layer thickness is 5 µm and the electroless plating rate is 10 µm per hour.

In the second test, a rapid prototype model of shark is electroless plated with nickel and the plating conditions and chemical compositions are the same as given in Table 3. The deposition starts immediately after the pre-treated acrylic resin sample is immersed into the electroless plating solution. Fig. 4 shows an acrylic resin prototype sample of the shark after immersing into the electroless solution for one hour. The lower part (grey) of the sample has a layer of coating while its upper part (black) shows the surface of neat resin. The coating is smooth and matte. The engraved words of "EXPLORE NZ" at the tail of the shark sample are still visible due to the uniform and thin deposition.

Table 3.
EDX elemental analysis of sample surface

| Element | Wt% | Atom% |
|---|---|---|
| Ni | 71.40 | 41.47 |
| P | 9.03 | 9.94 |
| O | 9.87 | 21.04 |
| C | 9.70 | 27.54 |

The EDS spectrum of the layer is given in Fig. 5. Four elements namely, nickel (Ni), phosphorous (P), carbon (C) and oxygen (O) are listed in the spectrum. The presences of carbon and oxygen are due to the acrylic resin underneath the micro thin nickel phosphorous layer while the hydrogen (H) is absent in the EDS spectrum, because the instrument limitation on low atomic number elements. Thus nickel and phosphorous are the major constituents of the coating. This is a good indication of the existence of the nickel-phosphorous alloy in the coating. Table 3 lists the percentages of the atom counts and weight. The actual percentages of nickel and phosphorous by weight are 89% and 11% respectively after ignoring the elements of oxygen and carbon which implies a high phosphorous content in the nickel-phosphorous alloy coating.

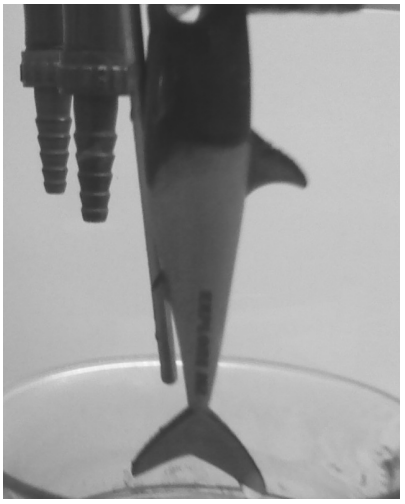

Fig. 4. The nickel layer on PerFactory™ RP model

It is reported that phosphorous has low solubility in nickel and causes lattice disorder in the crystalline nickel [17]. Hence, the molecular structure of the nickel-phosphorous alloy largely depends upon the amount of phosphorous. If the phosphorous content exceeds 8.5% by weight, the structure of the alloy will be amorphous because of the large lattice disorder caused by the phosphorous. Crystallographic structure of the coating was studied using automatic Philips XPERT-MPD PW3373 x ray diffraction system with Cu $K_\alpha$ radiation. Fig. 6 shows the x-ray diffraction pattern of nickel-phosphorous alloy (with 11% phosphorous) on the sample. Broad peaks at 2Theta = 20º and 2Theta = 45º in the Fig. 6 suggest an amorphous structure of the nickel-phosphorous alloy coating on the sample and thus the as plated layer is ductile. So it is clear that the layer structure is not pure crystal and further heat treatment can be employed to transfer amorphous structure in to crystalline structure[18]. According to JCPDS database, the peak representing at 45º corresponds to stable phase of nickel (JSPDS 04-0850 ) and that of at 20º corresponds to meta stable phase of nickel and phosphorous i.e. $Ni_5P_4$ (JSPDS 18-0883).

It is reported that phosphorous has low solubility in nickel and causes lattice disorder in the crystalline nickel [17]. Hence, the molecular structure of the nickel-phosphorous alloy largely depends upon the amount of phosphorous. If the phosphorous content exceeds 8.5% by weight, the structure of the alloy will be amorphous because of the large lattice disorder caused by the phosphorous. Crystallographic structure of the coating was studied using automatic Philips XPERT-MPD PW3373 x ray

diffraction system with Cu $K_\alpha$ radiation. Fig. 6 shows the x-ray diffraction pattern of nickel-phosphorous alloy (with 11% phosphorous) on the sample. Broad peaks at 2Theta = 20º and 2Theta = 45º in the Fig. 6 suggest an amorphous structure of the nickel-phosphorous alloy coating on the sample and thus the as plated layer is ductile. So it is clear that the layer structure is not pure crystal and further heat treatment can be employed to transfer amorphous structure in to crystalline structure[18]. According to JCPDS database, the peak representing at 45º corresponds to stable phase of nickel (JSPDS 04-0850) and that of at 20º corresponds to meta stable phase of nickel and phosphorous i.e. $Ni_5P_4$ (JSPDS 18-0883).

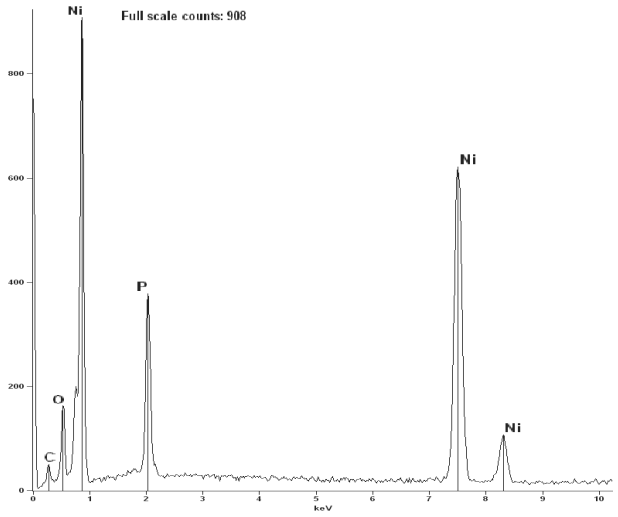


Fig. 5. The EDS analysis of the sample after immersing into the electroless solution

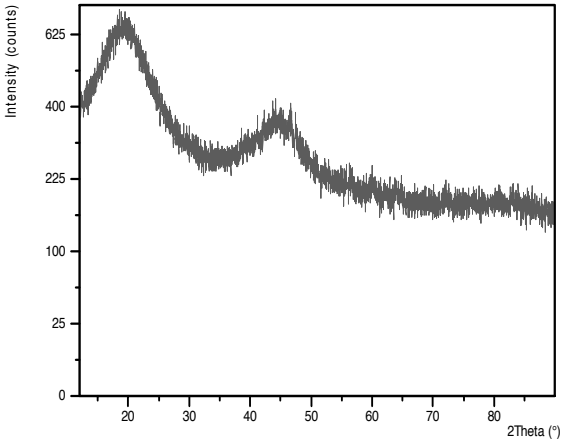


Fig. 6. The XRD pattern of the nickel-phosphorous alloy on the sample

The surface morphologies of the coatings revealed by SEM are shown in Figs. 7, 8, 9 and 10 with various magnification powers. Fig. 7 shows the coating with a magnification power of 60. Since the acrylic resin sample is prepared by the PerFactory™ rapid prototyping machine with layering technique, the stair effect is still visible after the electroless nickel plating on the sample. Furthermore, the gap between the bright lines (two arrows) in the Fig. 7 is measured to be 45 µm which is equal to the building layer thickness of the rapid prototype process Therefore, a pre-treatment such as polishing or sand blasting of the original prototype model surface can certainly enhance the surface smoothness of the final nickel phosphorous layer.

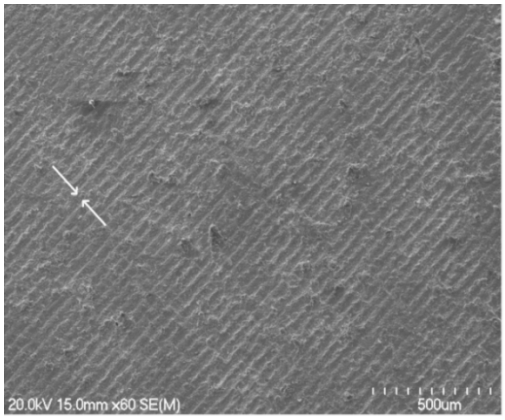


Fig. 7. SEM surface image (x60)

Fig. 8 presents the surface morphologies of the coating with a magnification power of 450. The spherical nodular structure of the nickel phosphorous alloy is shown in the Fig. 8 and approximate nodular diameters are range from 1 µm to 10 µm. Morphology of the structure also demonstrates homogeneity and the packing uniformity of electroless nickel layer.

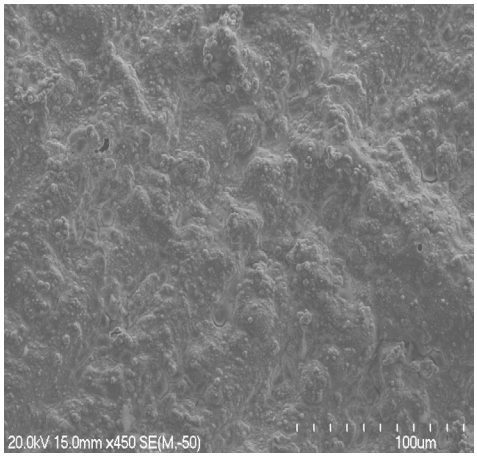


Fig. 8. The SEM surface image (x450)

The sample is then cut and viewed under the SEM. The image is shown in Fig. 9 with a magnification power of 800. The lower part of the image shows the acrylic resin while the cut cross section of the coating is seriously damaged with a lot of cracks and swells. However, there are no obvious flaws and apertures on the coating far away from the cut.

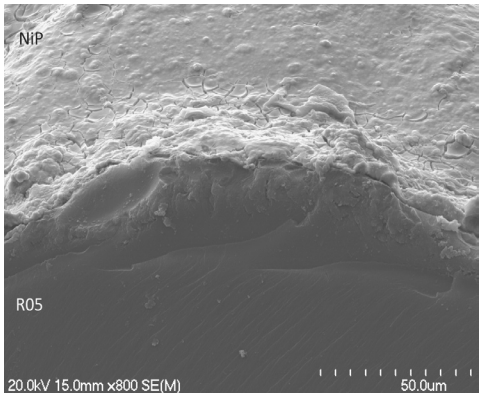


Fig. 9. SEM surface image at (x800)

a)

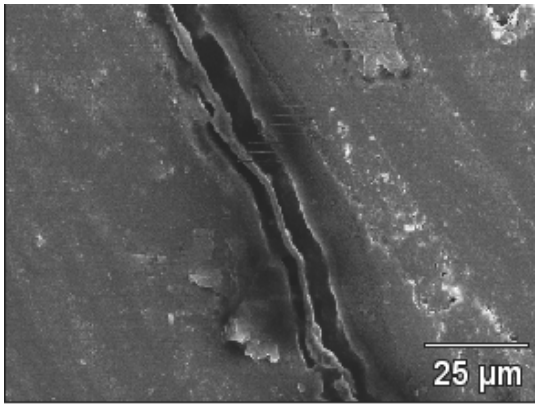


b)

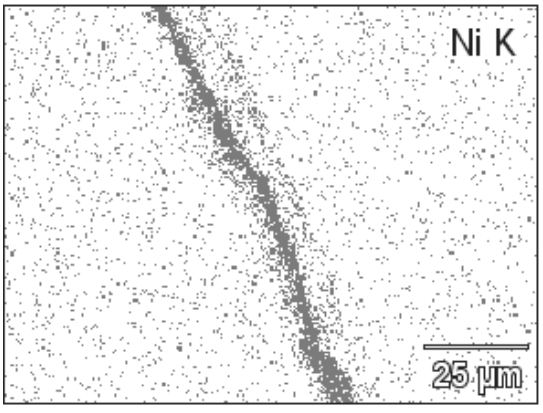


Fig. 10. Section image of: a) the layer, b) x ray mapping

In order to measure thickness of the layer, a cross section of the model is fabricated by cold curing epoxy resin. Surface of the cross section is ground with silicon sand papers and polish with rotary fabrics polisher. Then x ray map image of the cross section is obtained by EDS. Fig. 10 shows x ray map and SEM image of that cross section.

Thickness of the coating looks uniform, except some flattering out of the edges may be due to polishing. The layer trajectory is smooth. Surface irregularities of PerFactory™ model surface replicate same pattern of irregularities on the nickel layer. Approximate thickness of the layer is 2 µm after averaging measurements of thickness at several points of the SEM images. According to the x ray mapping image, nickel is distributed uniformly over the layer and nickel layer thickness value almost similar to 2 µm calculated above.

Surface hardness of the nickel coating is measured using Vickers micro hardness tester, Leco LM700. Data are collected for the load range from 10 gf to 1000 gf for both nickel coating and the uncoated PerFactory™ model using Vickers diamond indenter at 10 second dwelling time. Data are tabulated after getting the average of five readings for each loading condition in both cases. Fig. 11 shows the Vickers hardness comparison.

a)

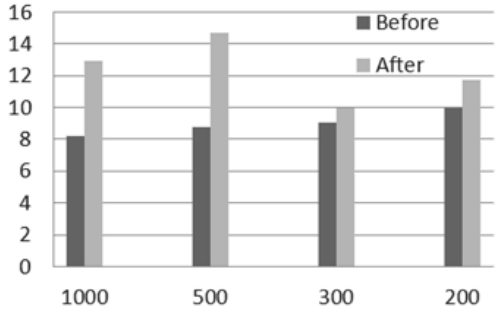


b)

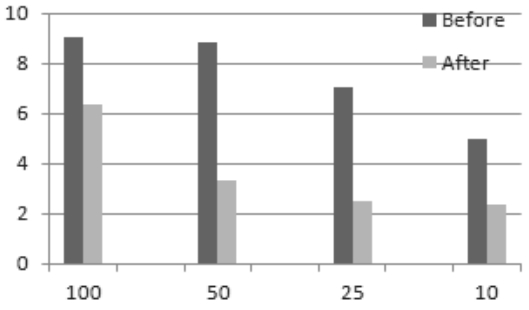


Fig. 11. Vickers Hardness value (HV) versus loading (gf): a) before, b) after the coating

According to the hardness data, the nickel coated surface has higher hardness value than the uncoated surface for the loading range from 1000 gf to 200 gf. The highest recorded Vickers hardness is 14.7 HV at 500 gf loading which is 83% higher than without coating hardness value of 8 $HV_{500\ gf}$.

The lowest value is 10 HV at 300 gf loading which is 11% higher than corresponding uncoated surface roughness value of 9 HV (at 300 gf). The variation of hardness value in this loading range is due to the local surface roughness effect and some experimental errors in setting up the sample and reading. However, it is clear enough to state that the nickel coating improves surface hardness of the PerFactory™ model.

On the other hand, hardness of the coated surface exhibit certain decreased in values in the load range from 100 gf to 10 gf. The highest fall is from 9 HV to 3 HV at 50 gf loading condition which means 66% lower hardness value of the coated surface than the uncoated surface. Therefore, this results show there is no improvement in the surface hardness of PerFactory™ model after nickel coating and contradict the result found in 1000 gf to 200 gf loading range.

Possible explanation for the contradicting result is the effect of surface roughness on low loading condition. For a low load of Vickers indenter, penetration depth of the indenter can be as small as from few nanometres to few microns depending on the material, load and indenter. Therefore, the surface roughness becomes effective as less material peeks hit the tip of the indenter. So the actual resistance for the indenter tip is low and the final reading is much less than the actual hardness of the material. Chung at. el. explains that penetration depth of an indenter must be sufficiently deep so that the surface response to the touching indenter tip behaves according to their bulk material properties[19]. To improve the valid of the hardness test, surface polishing can be employed which reduces the effect of surface roughness.

Therefore, Vickers hardness values for low loading condition in this experiment is not a reliable use in assessing the material hardness and Vickers hardness values for high load (1000 gf to 200 gf) can be considered.

## 4. Conclusions

Electroless plating is employed successfully to coat a layer of nickel-phosphorous alloy on the surface of an acrylic resin built PerFactory™ rapid prototype sample. Etching the surface before the activation has a significant effect on surface and creates anchor point for final layer. The EDS analysis shows that the major chemical composition of the layer is 89% nickel and 11% phosphorous by weight for the specified electroless solution and the plating conditions. The XRD pattern of the coating shows that the layer of nickel-phosphorous alloy is in amorphous status. The morphology study using SEM investigation is performed and surface morphology shows the homogeneous layer of nickel-phosphorous coating. Furthermore, new nickel coating improves the surface hardness of PerFactory™ model as much as 83%. However, further investigation is required to obtain mechanical and thermal properties of the layer for its functional applications.

## References


[1] R.E. Williams, S.N. Komaragiri, V. L. Melton, R.R. Bishu, Investigation of the effect of various build methods on the performance of rapid prototyping (Stereolithography), Journal of Material Processing Technology 61 (1996) 173-178.

[2] P.F. Jacobs, Rapid prototyping and manufacturing: fundamentals of stereolithography, Society of Manufacturing Engineering, Dearborn, 1992.

[3] D.E. Karalekas, Study of mechanical property of nonwoven fibre mat reinforced photopolymer used in rapid prototyping, Materials and Design 24 (2003) 665-670.

[4] L. Lu, Y.S. Choo, T. Miyazawa, Characteristics of photo polymeric material used in rapid prototypes, Mechanical properties in the green state, Journal of Material Processing Technology 67 (1997) 41-45.

[5] D. Karalekas, K. Ntoniou, Composite rapid prototype: overcoming the drawback of poor mechanical properties, Journal of Materials Processing Technology 153-154 (2004) 526-530.

[6] L. Libo, A. Maozhong, Electroless nickel-phosphorus plating on SiCp/Al composite from acid bath with nickel activation, Journal of Alloys and Compounds 461 (2008) 85-91.

[7] A. Malecki, A.M. Ilnicka, Electroless nickel plating from acid bath, Surface and Coating Technology 123 (2000) 72-77.

[8] X. Yin, L. Hong, B.H. Chen, T.M. Ko, Modelling the stability of electroless plating bath - diffusion of nickel colloidal particle from the plating frontier, Journal of Colloid and Interface Science 262 (2003) 89-96.

[9] Q. Zhang, M. Wu, W. Zhao, Electroless nickel plating on hollow glass microsphere, Surface and Coatings Technology 192 (2005) 213-219.

[10] Y. Xianghua, H. Wang, Z. Yang, P. Yin, X. Xin, XPS and AES investigation of two electroless composite coating, Applied Surface Science 158 (2000) 335-339.

[11] X. Tang, C. Bi, C. Han, B. Zhang, A new palladium free surface activation process for Ni electroless plating on ABS plastic, Material Letters 63 (2009) 840-842.

[12] H. Adachi, K. Taki, S. Nagamine, A. Yusa, M. Ohshima, Supercritical carbon dioxide assisted electroless plating on thermoplastic polymers, The Journal of Supercritical Fluids 49 (2009) 265-270.

[13] Q. Zhang, M. Wu, W. Zhao, Electroless nickel plating on hollow glass microspheres, Surface Coating and Technology 192 (2005) 213-219.

[14] S. Furukawa, M. Mehregany, Electroless plating of nickel on silicon for fabrication of high-aspect-ratio microstructures, Sensor and Actuators 56 (1996) 261-266.

[15] http:/www.envisiontec.de, accessed on 10.08.2011.

[16] G. Alexandre, T. Berthelot, P. Viel, A. Mesnage, P. Jegou, F. Nekelson, S. Palacin, ABS polymer electroless plating through a one-step poly acrylic acid covalent grafting, Applied Materials and Interfaces 2/4 (2010) 1177-1183.

[17] J.N. Balaraja, K.S. Rajam, Electroless deposition and characterization of high phosphorous Ni-P-$Si_3N_4$ composite coatings, International Journal of Electrochemical Science 2 (2007) 747-761.

[18] B. Bozzini, C. Martini, P.L. Cavallotti, E. Lanzoni, Relationships among crystallographic structure, mechanical properties and teratology behaviour of electroless Ni-P (9%)/$B_4C$ films, Wear 225-229 (1999) 806-813.

[19] S.M. Chung, A.U.J. Yap, Effect of surface finish on indentation modulus and hardness of dental composite restorative, Dental Material 21 (2005) 1008-1016.